

Fracture of disordered, elastic lattices in two dimensions

Hans J. Herrmann

*Service de Physique Théorique, Institut de Recherche Fondamentale, Commissariat à l'Energie Atomique,
Centre d'Etudes Nucleaires, F-91191 Gif-sur-Yvette CEDEX, France*

Alex Hansen

Institut für Theoretische Physik, Universität zu Köln, 5 Köln, 41, West Germany

Stephane Roux

*Laboratoire d'Hydrodynamique et de Mécanique Physique,
Ecole Supérieure de Physique et de Chimie Industrielles de la Ville de Paris,
10 rue Vauquelin, 75231 Paris CEDEX 05, France*

(Received 7 June 1988)

We study via simulation how a lattice breaks if each bond is an elastic beam having longitudinal and flexural breaking thresholds randomly selected according to various probability distributions. We observe scaling of force, displacement, and number of broken beams in the controlled regime. The distribution of local forces just before breaking is characterized by a multifractal spectrum $f(\alpha)$.

I. INTRODUCTION

How does a heterogeneous solid break when an externally applied displacement is slowly increased? This question is technologically of great importance, and an entire branch of material science is devoted to its study. Much empirical knowledge has been gathered and various theoretical approaches have been worked out.¹ However, there are still numerous fundamental aspects that remain unsolved.

In the last years a new way of approaching the problem has emerged from statistical physics, more precisely from the study of disordered media. The solid is modeled by a lattice of elastic bonds. Each bond represents the material on a mesoscopic level and it can break irreversibly if the strain applied at its ends exceeds a certain threshold. An essential feature of the model is the presence of quenched disorder either in the elastic constants, in the threshold values or in the presence of a bond (dilution). When an external strain (or stress) is applied to the lattice and then slowly increased, the individual bonds will break in a certain order until the system falls apart. The sequence of breaking bonds and the spatial patterns they form are supposed to mimic a real breaking process. They depend on the type of disorder and on its distribution. But how relevant is this dependence? Is there some universal law common to all distributions? This is the typical question in statistical physics that one is interested to answer. Also other quantities like the total number of bonds that one must break or the maximum stress one has to apply to break the system apart might follow some universal laws. It is in this direction that we aim the present work.

The simplest way of describing an elastic solid is via the electric analog,² i.e., to reduce the problem to a scalar one. The bias that is introduced through this simplification in the case of dilution is now well under-

stood.³ In this approach the bonds of the lattice are fuses. Disorder has been considered in the conductivities,^{4,5} in the lattice in form of dilution^{6,7} and in the thresholds.⁸ It has been found that the distribution of external breaking voltages⁹ and the maximum voltage drop across a bond¹⁰ follow nontrivial laws.

The results obtained for the electrical analog can serve as a guideline but if one wants to compare theory and experiment it is inevitable to consider the vectorial nature of elasticity on one hand and the bond-bending effects³ on the other. Some cases of fracture that include randomness and take into account the vectorial nature have been studied but they are relevant to very particular situations only. In one case a thin layer of elastic-brittle material connected to a rigid substrate, where breaking is thermally activated, has been investigated numerically by Meakin.¹¹ The other case is the mechanical analog of dielectric breakdown,¹² and its experimental relevance is not clear. This approach gives rise to fractal patterns and has been attempted¹³ using a discretization of Lamé's equation.

In the present paper, we consider the most common situation where fracture takes place in the bulk of the material. We will take into account the vectorial nature of elasticity and thus bond-bending by using the beam model.¹⁴ In this model each bond of the lattice is an elastic beam soldered on both ends to sites. In two dimensions each site has three degrees of freedom: two spatial coordinates and an angle of rotation. The rotation of a site necessarily curves and shears its adjacent beams [see Fig. 1(a)]. Elongation, shear or flexion of a beam cost energy. In addition, we give in our model to each beam a breaking criterion with randomly chosen threshold values. This means that we choose the quenched disorder to be in the breaking thresholds. In the next section we will describe the model and the algorithm that we use to solve it. In the following section we present and discuss our results.

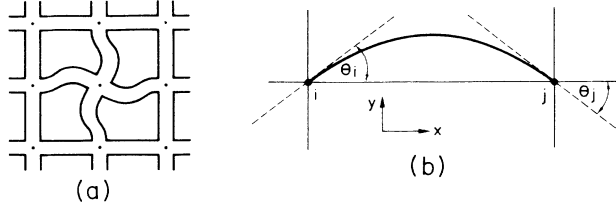


FIG. 1. Schematic representation of the beam model (a) rotation of one site (b) beam flexed due to the angles at its extremities.

II. MODEL AND METHOD

We consider a square lattice of size $L \times L$ with periodic boundary conditions in the horizontal direction and fixed boundary condition on top and bottom. On each site i there are three continuous degrees of freedom: the two coordinates x_i and y_i and $z_i = \theta_i l$ where $\theta_i \in [-\pi, \pi]$ is an angle and the lattice spacing l is set to be unity. Nearest-neighboring sites are connected through a “beam” in such a way that it forms an angle θ_i with the direction of the underlying square lattice at the site i [see Fig. 1(b)].

A beam is to be imagined having a certain thickness giving it not only longitudinal but also shear elasticity. Its elastic behavior is given, e.g., in Ref. 15 and for our purposes also in Ref. 14: One defines the three material-dependent constants

$$a = \frac{l}{EA}, \quad b = \frac{l}{GA}, \quad c = \frac{l^3}{EI}, \quad (1)$$

where E and G are the Young and shear moduli, A is the area of the beam section, and I is the moment of inertia for flexion. Then one has for a horizontal beam between sites i and j [Fig. 1(b)] for the longitudinal force:

$$F = \frac{1}{a}(x_i - x_j), \quad (2)$$

for the shear force:

$$S = (b + \frac{1}{12}c)^{-1}[y_i - y_j + \frac{1}{2}(z_j + z_i)], \quad (3)$$

and for the flexural torque at site i :

$$M_i = \frac{b}{c(b + \frac{1}{12}c)}(z_i - z_j) + \frac{1}{2}(b + \frac{1}{12}c)^{-1} \left[y_i - y_j + \frac{2}{3}z_i + \frac{z_j}{3} \right]. \quad (4)$$

Analogous formulas are valid for vertical beams. In Eqs. (2)–(4) we only consider the leading linear terms. This is an approximation if the local strain is not infinitesimal. However, we consider here the case of a brittle material for which a linear approximation is valid up to the threshold. In this work we arbitrarily chose $a = 1$, $b = 30/7$, and $c = 2b$ as material constants.

In first order, only two mechanisms contribute to the breaking of a beam: elongation and flexion. We therefore introduce only two threshold values t_F , for elonga-

tion and t_M , for flexion randomly chosen for each beam. The thresholds are picked according to the following probability distributions:

$$P(t_F) = (1-x)t_F^{-x} \quad \text{with } t_F \in [0, 1]$$

and (5)

$$P(t_M) = (1-x)q^{x-1}t_M^{-x} \quad \text{with } t_M \in [0, q],$$

where the exponent $x < 1$ and the relative width q of the distributions are parameters of the model. Large disorder is given by $x \lesssim 1$, small disorder by negative x . We then use for a beam the following rupture criterion¹⁶ that can be derived from Tresca’s or von Mises’s general yielding criteria for the material the beam is made from: The beam breaks if

$$\left(\frac{F}{t_F} \right)^2 + \frac{\max(|M_i|, |M_j|)}{t_M} \geq 1. \quad (6)$$

To impose an external strain we attach at the bottom a zeroth line on which for all sites $x_i = y_i = z_i = 0$ are fixed and on top we attach a $(L+1)$ th line on which all sites have the same fixed values $x_i = X$, $y_i = Y$, and $z_i = 0$. If we want an external elongation we set $X = 0$ and $Y = 1$ and if we want an external shear we set $X = 1$ and $Y = 0$. The fact that we fix the external strain to be unity is no restriction. This is because all the microscopic quantities of the lattice (displacements, forces, etc.) are proportional to this value. It is the aim of our calculation to determine this proportionality constant λ such that one would just break the first (weakest) beam. That means that we look for the beam between sites i and j for which the λ that satisfies in Eq. (6) the equality

$$\left(\frac{F\lambda}{t_F} \right)^2 + \frac{\max(|M_i\lambda|, |M_j\lambda|)}{t_M} = 1 \quad (7)$$

is smallest. The force F and the moments M_i and M_j in Eq. (7) are obtained for a unit external strain.

In other words we calculate for fixed unity external displacement the values for x_i , y_i , and z_i on each site of the lattice and from there we calculate for each beam

$$\lambda = \frac{(h_1^2 + 4h_2)^{1/2} - h_1}{2h_2} \quad (8)$$

with $h_1 = \max(|M_1|, |M_2|)/t_M$ and $h_2 = (F/t_F)^2$ using Eqs. (2) and (4). The beam that has the smallest value of λ “breaks” and is removed [i.e., its constants a , b , and c in Eq. (1) become infinite]. A beam that has been removed will never be restored. Once a beam has been removed all the values of x_i , y_i , and z_i on the lattice will change and must be calculated again in order to determine via the same procedure the next beam that will break. In this way starting from a finite square lattice that has a beam on each bond one gradually removes the beams one by one in a sequence that depends on the randomly distributed threshold values through the procedure described above. We assumed implicitly in this model that the network relaxes to mechanical equilibrium at a much faster rate than the bond breaking process.

TABLE I. Number N of lattices generated for the case $x=0$, $q=1$, external elongation for different sizes L .

L	N
4	50 000
8	10 000
16	500
32	40
64	1

When the last beam breaks for which top and bottom were still connected via beams the system falls apart and the breaking procedure is stopped. We call n_f the total number of beams that had to be broken to reach that point. After this point all λ would trivially be infinity.

The calculation of the x_i , y_i , and z_i on the sites before each breaking is done numerically via relaxation using the conjugate gradient method.^{17,18} More precisely we use Eqs. (40)–(46) of Ref. 18 replacing the kernel \vec{D} by:

$$\sum_j \vec{D}_{ij} \begin{pmatrix} x_i \\ y_i \\ z_i \end{pmatrix} = \alpha \begin{pmatrix} F^I - S^{II} - F^{III} + S^{IV} \\ S^I + F^{II} - S^{III} - F^{IV} \\ M_i^I + M_i^{II} + M_i^{III} + M_i^{IV} \end{pmatrix}, \quad (9)$$

where I–IV indexes the four beams adjacent to the site i . We stopped after reaching a precision of $\epsilon = 5 \times 10^{-7}$ [see Eq. (47) in Ref. 18]. We did not use Fourier acceleration since even for the largest lattices we studied ($L=64$) it was inefficient. The number of relaxation steps needed grows roughly as $L^{2/3}$ and the CPU time to break a lattice apart grows like $L^{4.3}$.

In order to properly handle the quenched disorder in the breaking thresholds we repeated the calculation N times with different casts of thresholds and all the quantities that we calculated are averages over the N samples. These averages were always taken for fixed number of broken bonds. In Table I we show typical values for N .

III. THE BREAKING CHARACTERISTICS

During the breaking process we monitor a certain number of quantities. In the simulation we imposed an external displacement of unity. Therefore the real total external elongation or shear (depending on the initial condition), i.e., the one needed to break a beam, is just the λ from Eq. (8). Similarly $Y = \sum_i F_i$, where the sum goes over all the vertical beams that connect lines zero and one, is the elastic modulus of the lattice which could also be obtained from the computation of the total energy of the system. λ and Y are averaged over many samples. The total external force f that must be applied to break a beam is then given by $f = \lambda Y$.

The force-displacement characteristic, i.e., f versus λ , at the breaking of the individual beams is experimentally accessible and contains the most interesting information about the breaking process. In Fig. 2 we show this characteristic for different sets of parameters. One can see that in the beginning of the rupture process force and displacement increase proportional to each other. We call this the ‘‘controlled’’ regime.

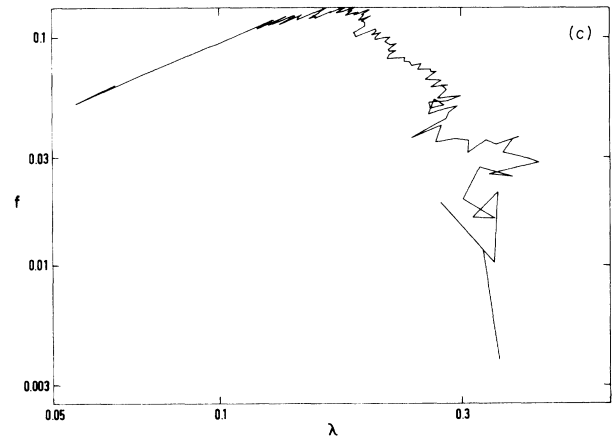
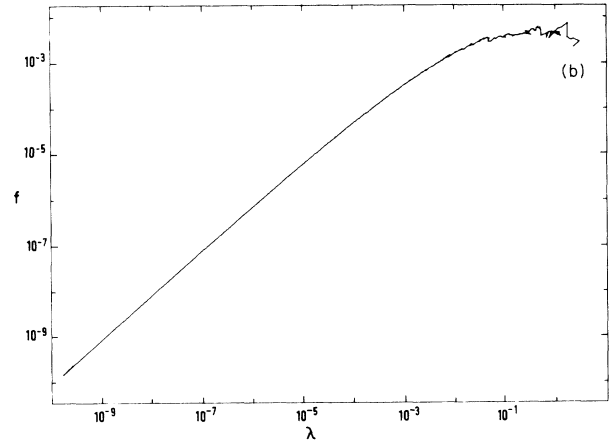
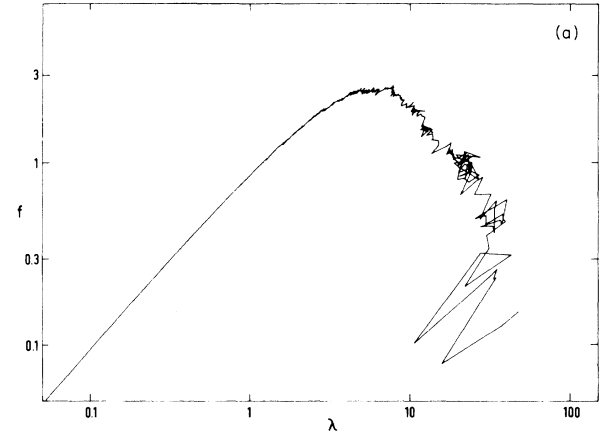


FIG. 2. Log-log plot of the force f against the displacement λ at the rupture of the individual beams applying an external elongation for $L=16$ (a) $x=0$, $q=1$, $N=60$; (b) $x=0.8$, $q=1$, $N=30$; (c) $x=0$, $q=0.01$, $N=100$.

In this region the statistical fluctuations are weak. It is dominated by the disorder: if one has more disorder (larger x) the region is larger [compare Figs. 2(a) and 2(b)]. At some point one reaches a maximum in f . The value of this maximum is the force needed to break the system apart. After going through the maximum there is a second region: the catastrophic rupture. One needs each time less force to break the next beam. This region has big statistical fluctuations. Experimentally it is only accessible if one imposes the external strain and not if one imposes the external stress because in the second case all bonds will break simultaneously in the catastrophic regime.

It is of interest to analyze these characteristics further to study the dependence on the size L . Unfortunately, specially for large L , the statistical noise is substantial. For this reason we wrote a smoothing routine that makes use of the obvious fact that λ must monotonically increase in the process and that f cannot have minima if one would have averaged (in the way described above) over infinitely many samples. So if, for example, in our data we had at two subsequent breakings λ and λ' with $\lambda' < \lambda$ (where these data are the averages over a finite number of samples) we replaced them by $\lambda \rightarrow \frac{1}{4}\lambda + \frac{3}{4}\lambda'$

and $\lambda' \rightarrow \frac{2}{3}\lambda + \frac{1}{3}\lambda'$. An example of how this smoothing works is shown in Fig. 3.

By conveniently scaling the axis of the characteristics we tried to collapse the data for different L . The collapse works best in the controlled region for:

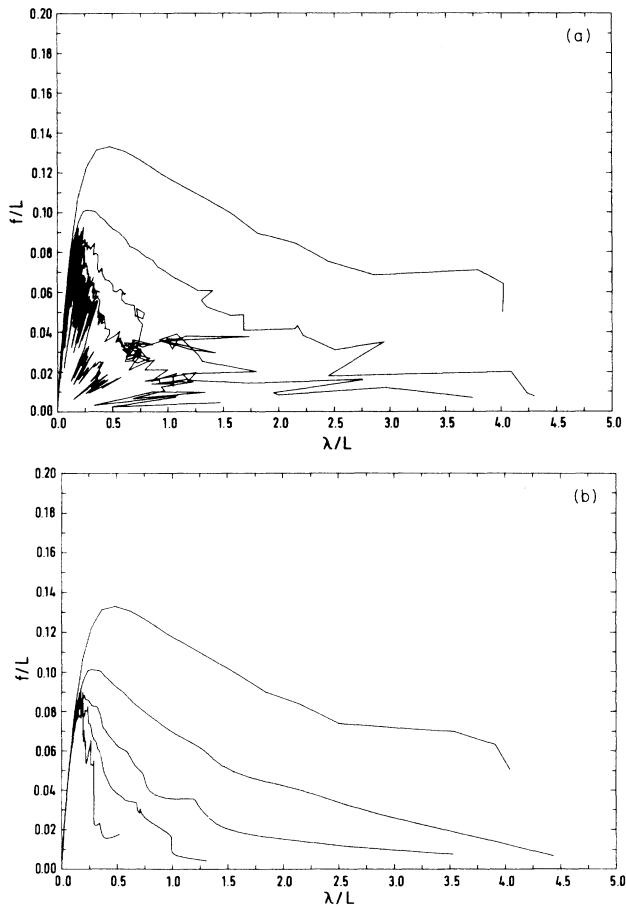


FIG. 3. f/L against λ/L for $x=0$, $q=1$ applying an external elongation for different sizes L (a) raw data, (b) using the smoothing routine.

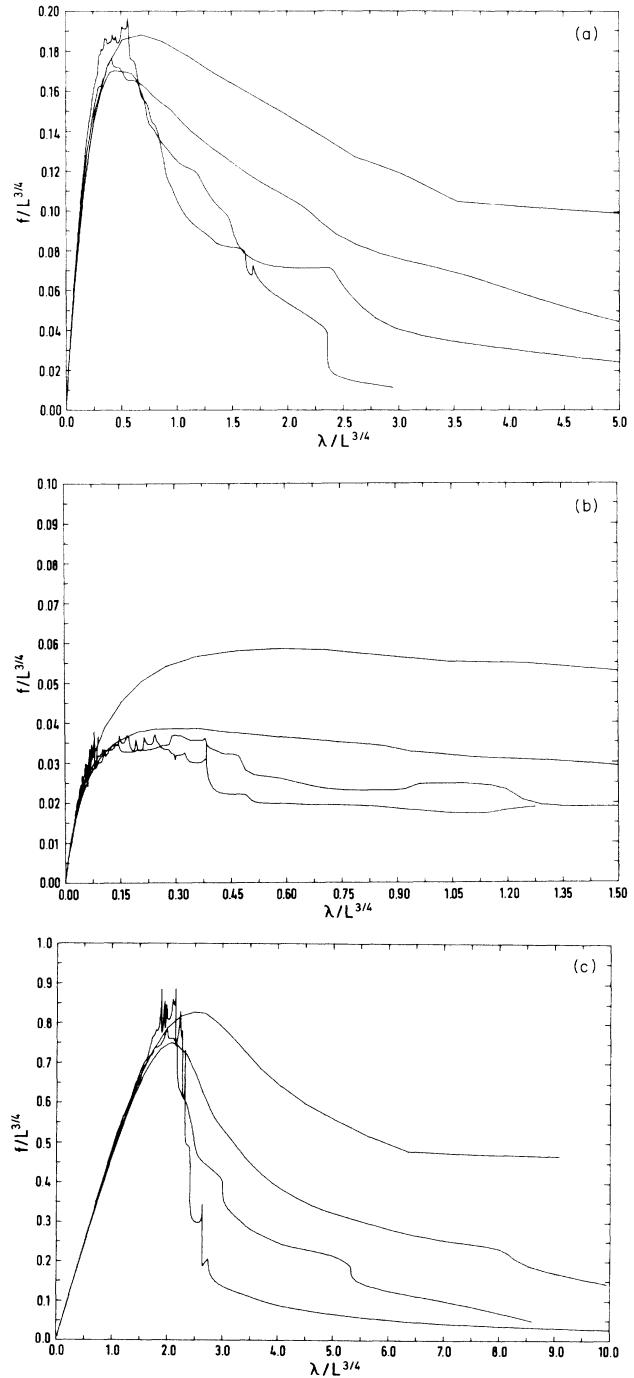


FIG. 4. $f/L^{3/4}$ against $\lambda/L^{3/4}$ for different sizes for (a) external elongation, $x=0$, $q=1$; (b) external elongation, $x=0.5$, $q=1$; (c) external shear, $x=0$, $q=1$ (data smoothed).

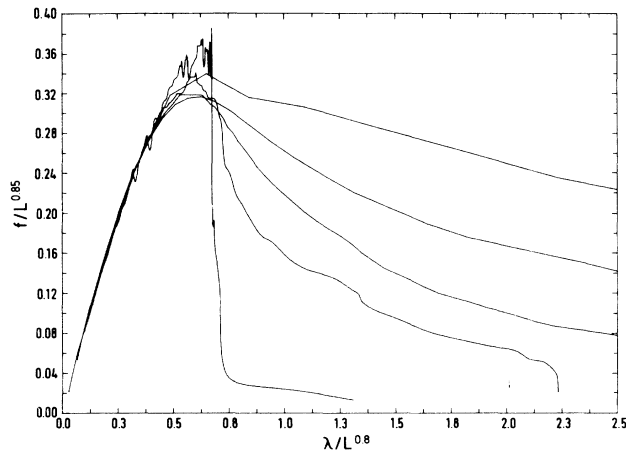


FIG. 5. $f/L^{0.85}$ against $\lambda/L^{0.8}$ for different sizes for an external elongation $x = -1$ and $q = 1$.

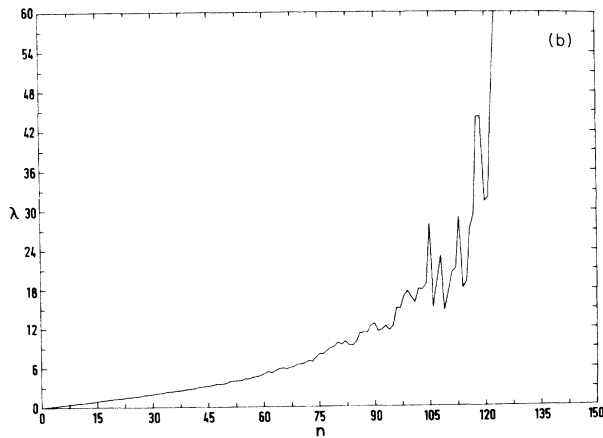
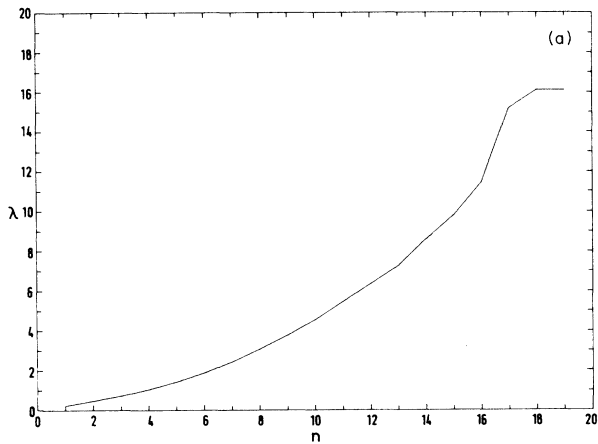


FIG. 6. Elongation λ against number n of broken beams for an external elongation, $x = 0$, $q = 1$ for (a) $L = 4$ and (b) $L = 16$.

$$f = L^{3/4} \phi(\lambda L^{-3/4}) \quad (10)$$

where ϕ is a scaling function while the brittle regime does not scale as shown in Fig. 4. This is true for $x \geq 0$; for $x = -1$ we found better collapse for somewhat larger exponents (see Fig. 5). Our exponents have error bars of about 10%. We also tried to collapse the data using a scaling law of the type $L^\alpha (\ln L)^\beta$ and found that the pure powerlaw scales the data best. It is specially remarkable that a scaling with $L/\sqrt{\ln L}$ does not work at all since this type of behavior has been calculated in the scalar case for dilution⁷ and for distributions in the threshold with a lower cutoff⁸ for the maximum of the characteristic. The fact that f and λ scale in the same way implies that the elastic modulus $Y = f/\lambda$ is independent of L .

Another quantity that should be observed is the number n of beams that have been broken at a certain stage of the process averaged over several samples. In Fig. 6 we show the elongation λ as a function of n . Again one can scale the data and again the scaling works in the controlled and not in the brittle regime. In Fig. 7 we see that a scaling of the form

$$n = L^\gamma \psi(fL^{-3/4}), \quad (11)$$

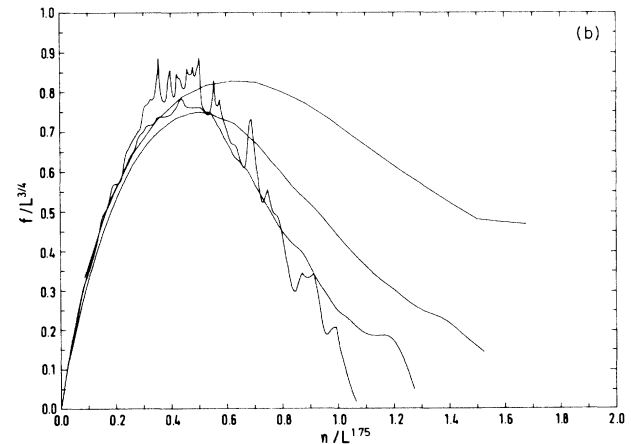
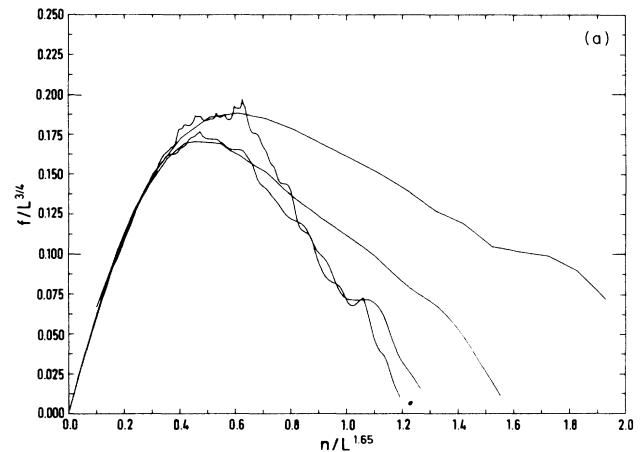


FIG. 7. Data collapse of $f/L^{3/4}$ against n/L^γ for different sizes for $x = 0$, $q = 1$ (a) external elongation; (b) external shear.

where ψ is a scaling function, works well and we have for $x=0$, $q=1$, $\gamma=1.65$ for an external elongation and $\gamma=1.75$ for an external shear. For $x=0.5$, $q=1$ and an external elongation we obtained $\gamma=1.85$. The error on γ is about 10%.

A particularly important point of the breaking characteristic is of course the maximum after which the system will break catastrophically. The maximum characterizes macroscopic brittle fracture. We analyze in Fig. 8 the

force f_b , the displacement λ_b and the number of broken beams n_b at the maximum. f_b is the average over the individual maxima of each sample while λ_b and n_b are the values at the maxima of the averaged curves. We see that n_b clearly follows a powerlaw in L with an exponent of about $\frac{7}{4}$. This value seems quite universal since in Fig. 8 we show it to be valid for large disorder ($x=0.5$) and very small disorder ($x=-1$) and for external elongation

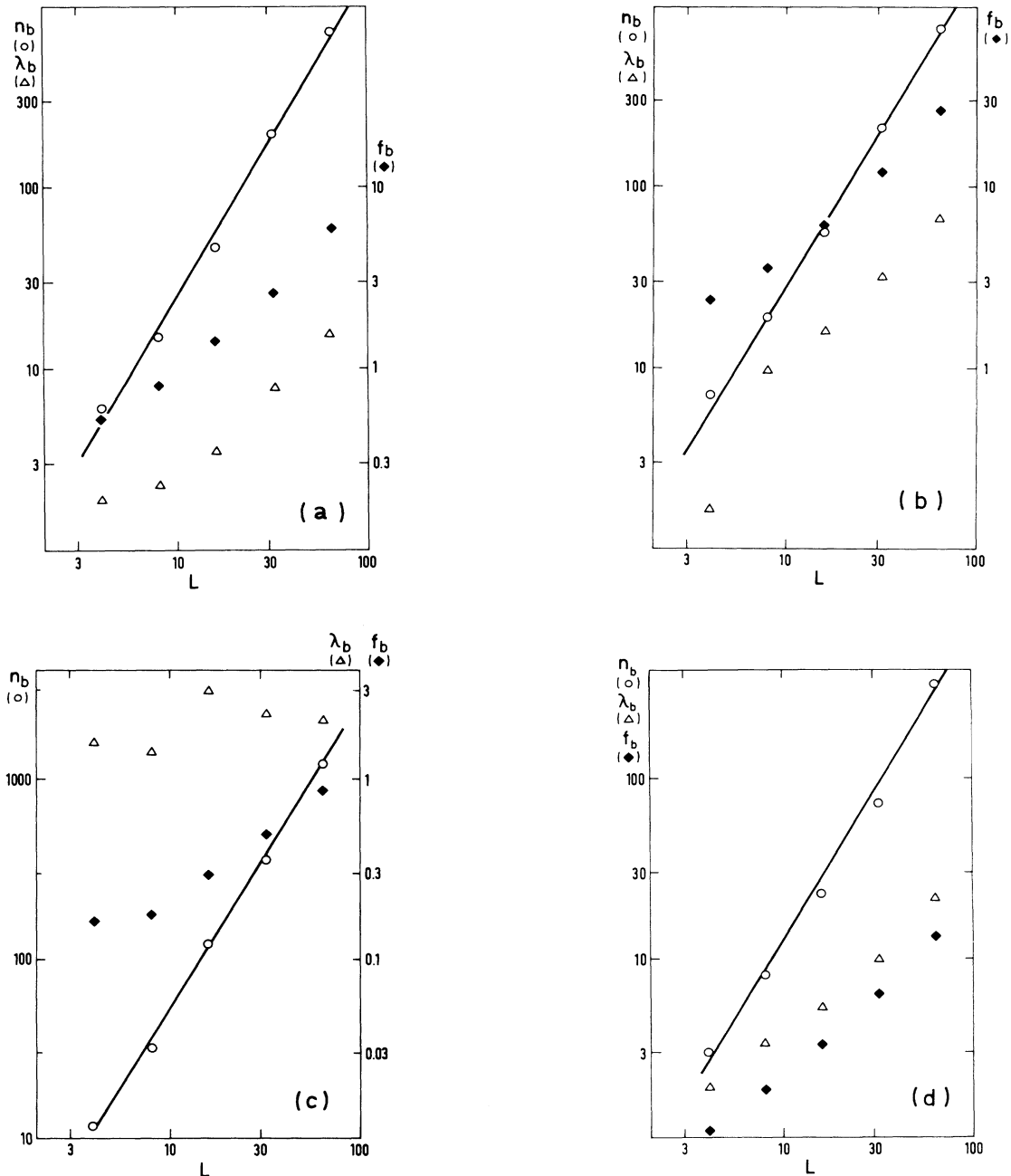


FIG. 8. Log-log plot of n_b (\circ), λ_b (Δ), and f_b (\blacklozenge) as a function of L for (a) $x=0$, $q=1$, external elongation; (b) $x=0$, $q=1$, external shear; (c) $x=0.5$, $q=1$, external elongation; (d) $x=-1$, $q=1$, external elongation. The straight line is a guide to the eye of slope $7/4$.

as well as external shear. This result is in contrast to what is found if the probability distribution of breaking thresholds has a lower cutoff;⁸ then it can be shown that n_b is a finite number independent on L . Force f_b and displacement λ_b do not lie on a straight line in Fig. 8 so that they do not follow a pure powerlaw. The curvature in the data can be due to strong corrections to finite-size

scaling or to logarithmic prefactors. The precision of the data and the small sizes considered do not allow us to distinguish between these possibilities. It is nevertheless clear from the data that λ_b is not compatible with a behavior $L/\sqrt{\ln L}$ as found in similar cases^{7,8} because the effective slope in Fig. 8 is already larger than unity at the larger sizes and the curvature is positive. Another fact

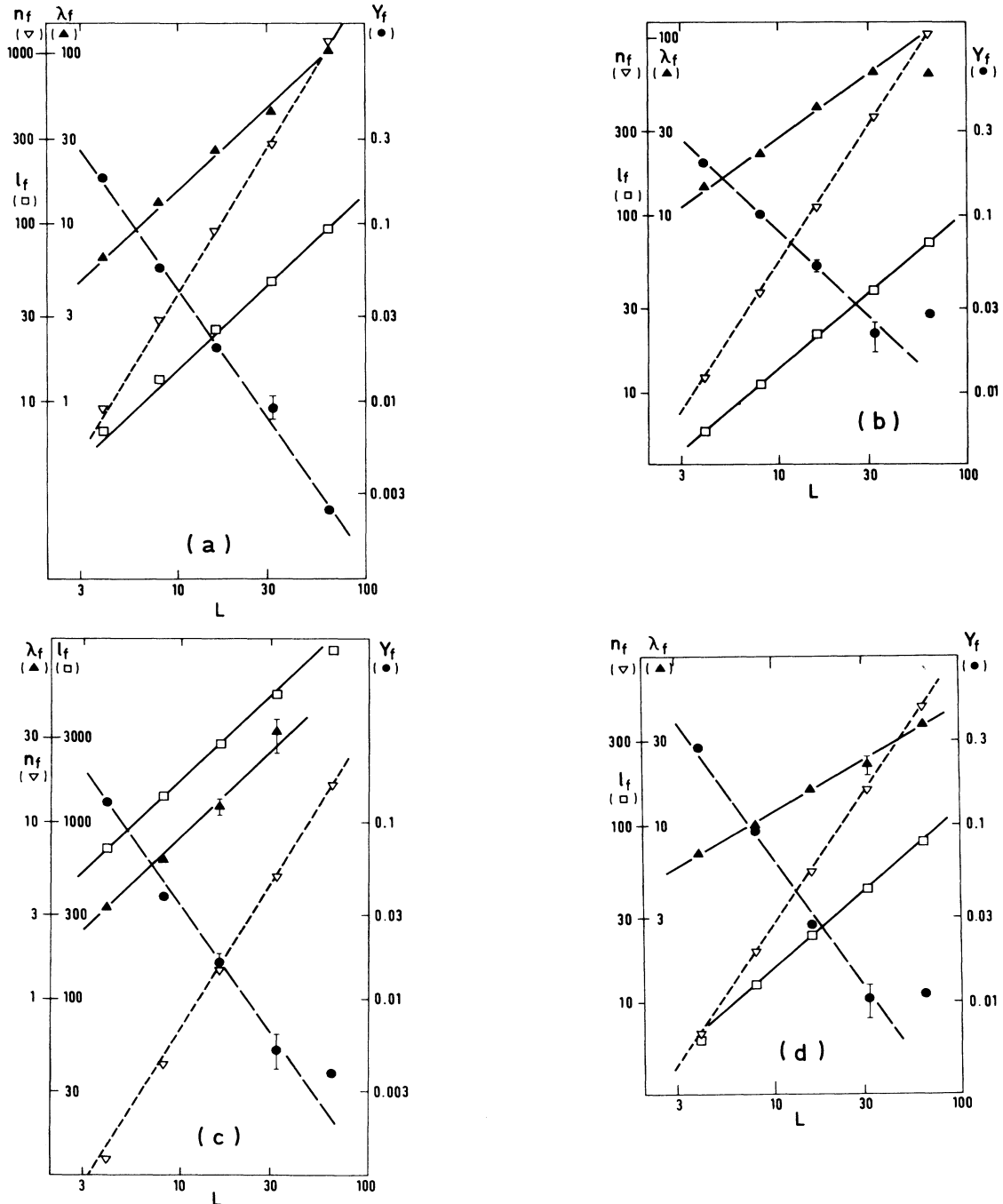


FIG. 9. Log-log plot of n_f (∇), λ_f (\triangle), Y_f (\bullet), and l_f (\square) as a function of L for (a) $x=0$, $q=1$, external elongation; (b) $x=0$, $q=1$, external shear; (c) $x=0.5$, $q=1$, external elongation; (d) $x=-1$, $q=1$ external elongation. In (a) and (c) the solid lines have slope 1, the dashed lines slope $-3/2$ and the dotted lines slope $7/4$. In (b) we have slopes 1.64, 0.76, -1 , and 0.9 for n_f , λ_f , Y_f , and l_f and in (d) we have slopes 1.55, 0.61, 1.5, and 0.9 for n_f , λ_f , Y_f , and l_f .

that can be extracted from the data is that like in the controlled regime f_b and λ_b have essentially the same L dependence which means that the elastic moduli Y_b are independent of L within the statistical error bars.

The other special point of the breaking process is the end of the characteristics, i.e., when the last beam breaks before the system falls apart. This point gives information about the catastrophic rupture. The average number n_f of broken beams at this point scales (similar to the maximum) roughly like $L^{7/4}$ as shown in Fig. 9; in some cases [Figs. 9(b) and 9(d)] the exponent is a little smaller. In fact n_b and n_f are quite parallel which means that the number $n_f - n_b$ of beams broken during the catastrophic break also scales roughly like $L^{7/4}$. This is in contrast to the result obtained for the single crack approximation⁸ which predicts an n_f proportional to L . The average displacement λ_f at the final breaking point increases with a powerlaw in L where the exponent is less or equal to unity depending on the case. The behavior of the average Young modulus Y_f at this point is interesting. It decreases like $L^{-3/2}$ for an external force and like L^{-1} for an external shear. The exponents have an uncertainty of nearly 10%. Finally we also calculated the average chemical distance at the final breaking point, i.e., the length of the shortest path if one goes from top to bottom over present beams. This length scales like L and is therefore not fractal.

IV. LOCAL PROPERTIES

During the process of rupture there are very strong local strains specially at the tips of cracks. The study of these local effects seems crucial to understand the mechanisms of rupture. Experimentally local properties might eventually be accessible, for instance through photoelastic measurements.

We have analyzed the two terms $h_2^* = (F/t_F)^2$ and $h_1^* = \max(|M_1|, |M_2|)/t_M$ that appear in Eq. (8), at the beam that breaks averaged over the samples. The behavior of h_2^* as a function of n is shown in Fig. 10 for two different sizes. We see that it varies over many orders of magnitude. In the beginning of the process h_2^* is very large due to the very small values of t_F which determine the breaking; so there the process is controlled by the disorder. In Fig. 11 we see the behavior of h_1^* . Both h_1^* and h_2^* decrease monotonically and this has as consequence the monotonic increase of λ . But we see that h_1^* decreases very slowly so that it is actually the elongation given by h_2^* which dominates the behavior of λ as a function of n . h_1^* fluctuates more or less equally strong during the whole process and is comparable in size and fluctuation to the behavior of h_2^* at the end of the process. So, only at the end the two contributions become about equally relevant.

To see better the two contributions to breaking, elongation and flexion, we regard $f_c = \lambda(h_2^*)^{1/2}$ and $m_c = \lambda h_1^*$ for different system sizes. We would expect $f_c^2 + m_c = 1$ if we would have calculated f_c and m_c for each sample and then averaged, but we averaged first λ and the h^* 's and then took the product. In Fig. 12(a) we

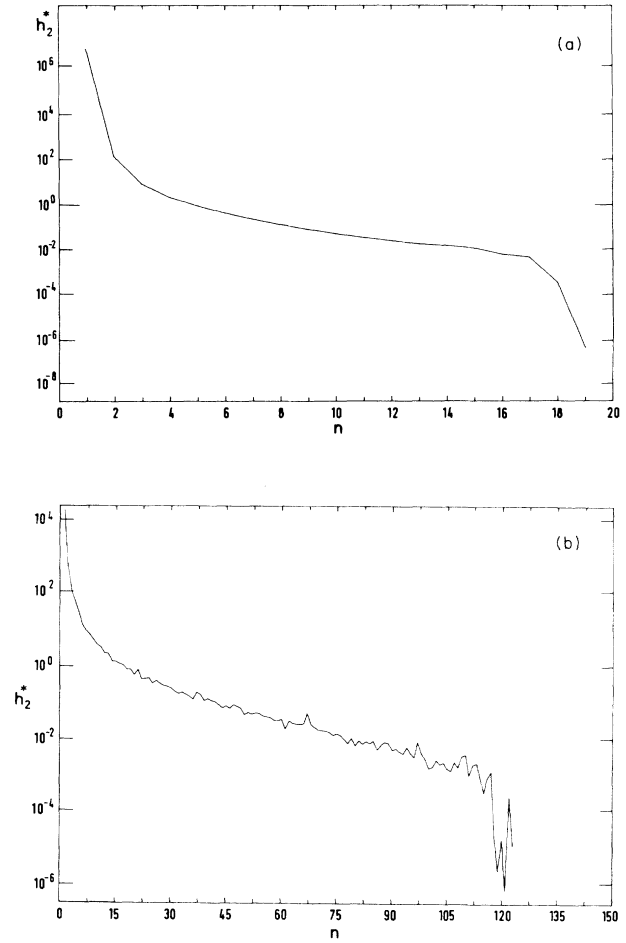


FIG. 10. h_2^* logarithmically plotted against the number n of broken beams for $x=0$, $q=1$ and external elongation for (a) $L=4$ and (b) $L=16$.

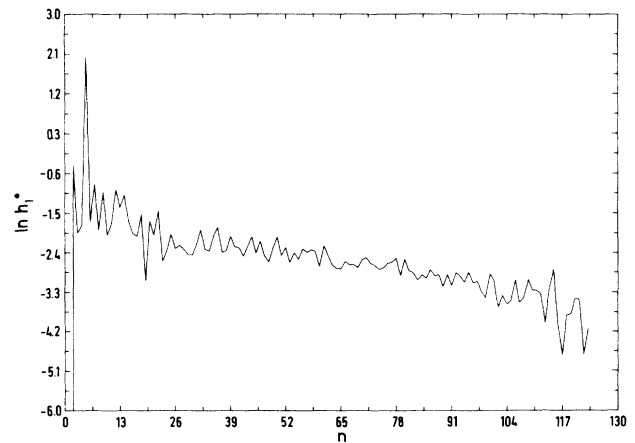


FIG. 11. h_1^* logarithmically plotted against n for $x=0$, $q=1$, $L=16$, and an external elongation.

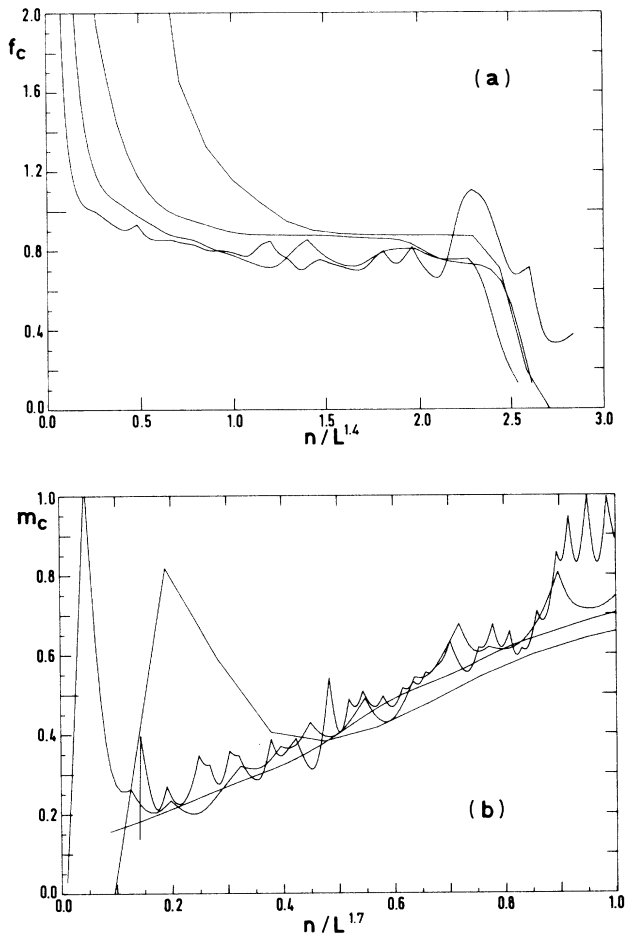


FIG. 12. f_c (a) and m_c (b) as function of $n/L^{1.4}$ for $x=0$, $q=1$, external elongation for various system sizes.

see f_c , the contribution of elongation to the breaking, monotonically decreasing. It is interesting to note, that in the catastrophic regime all curves collapse if n is scaled like $L^{1.4}$. The data all fall on a plateau of about one in the intermediate region. The behavior of m_c is seen in Fig. 12(b). As expected it is more or less complementary to the behavior of f_c , i.e., monotonically increasing and with the same scaling behavior.

The situation of the system just before it breaks completely apart is particularly interesting since all the force is transmitted through a very complex and weakly connected substructure of stressed beams. We therefore analyzed this situation a little further under the aspect of Ref. 19, i.e., via the distribution $n(F)$ of the local forces and $n(S)$ of the local shears that are applied on each beam, measured at constant unity displacement where the average is now taken over all the configurations for which the system breaks apart when the next bond is removed.

A particularly useful way to plot these histograms has turned out to be the $f(\alpha)$ spectrum.^{20,21} One defines the exponents

$$\alpha = \frac{\ln F - c_1}{\ln L} \quad (12)$$

and

$$f(\alpha) = \frac{\ln n(F) - c_2}{\ln L} \quad (13)$$

where the constants c_1 and c_2 are amplitudes. α describes how singular a certain region of beams is, i.e., how the stress would change if the size of the system increases. $f(\alpha)$ is the fractal dimension of the subset of beams having a singularity of strength α . The values of c_1 and c_2 are given through the scaling in L , i.e., they must be chosen such that for large L all $f(\alpha)$ curves collapse on a single curve. Then the scaling $F = e^{c_1} L^\alpha$ and $n(F) = e^{c_2} L^{f(\alpha)}$ is fulfilled.

In Fig. 13 we show $f(\alpha)$ where c_1 and c_2 have been chosen just in the way described above, but the determination of c_1 and c_2 is not very precise since it is difficult to know what the behavior for large L will be: Our systems are quite small for this analysis. Still one sees that the collapse is reasonable. Since the number n_f of bonds cut just before the system breaks completely apart goes like $n_f \sim L^\gamma$ with $\gamma < 2$ it is clear that the total

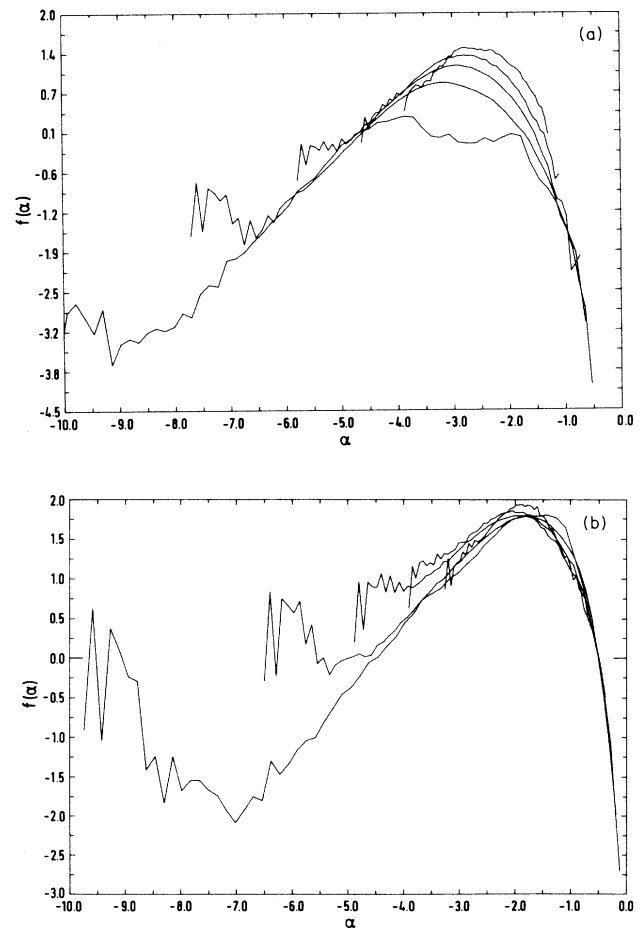


FIG. 13. Multifractal spectrum, i.e., $f(\alpha)$ against α for the distribution $n(F)$ of forces F . We show data for $L=4, 8, 16, 32$, and 64 . For $x=0$, $q=1$ and (a) external elongation with $c_1=c_2=0$ and (b) external shear with $c_1=2.5$ and $c_2=2.0$.

structure just before breaking is not fractal and so the largest value of $f(\alpha)$ must be $f_{\max}=2$. The convergence towards 2 is studied in Fig. 14 for the case of Fig. 13(a). We verify the expected behavior as $1/\ln L$ which indicates that we have chosen the right values of c_1 and c_2 . The value of α at this maximum is about -2 which means that the majority of beams have a stress scaling as L^{-2} .

In Fig. 13 we also see that for increasing system sizes L the end of weak singularities (left-hand side) saturates each time towards higher values and it cannot be excluded that for $L \rightarrow \infty$ they will stay at 2. Such a scenario for the “cold” side of the spectrum has previously been proposed²² for the random resistor network.

The “hot” side of the spectrum and the form of the maximum in Fig. 13 seem quite stable towards changes in L and it is very probable that one obtains asymptotically for large L a curved $f(\alpha)$ spectrum. This means that one has multifractality,²¹ i.e., an infinity of relevant exponents determining the scaling behavior of the structure.

In Fig. 15 we show the analog of Fig. 13 for the distribution of local shears, i.e., replacing in Eq. (12) and (13) F by S . Qualitatively the situation is similar to the case of local forces but the spectra are a little less curved and less smooth. One cannot exclude the possibility that they might tend towards two joined straight lines in this case.

Another way to investigate the distribution $n(F)$ and look for multifractality is via the moments:¹⁹

$$m_k = \sum_i (F_i)^k n(F_i) \tag{14}$$

where the sum runs over all the beams i . These moments should scale like¹⁹

$$m_k \sim L^{f(\alpha)+k\alpha} \tag{15}$$

We calculated m_k for various values of k and the size dependence is shown in Fig. 16. The zeroth moment beautifully scales like L^2 reconfirming that $f_{\max}=2$. the first negative moment scales with an exponent larger than

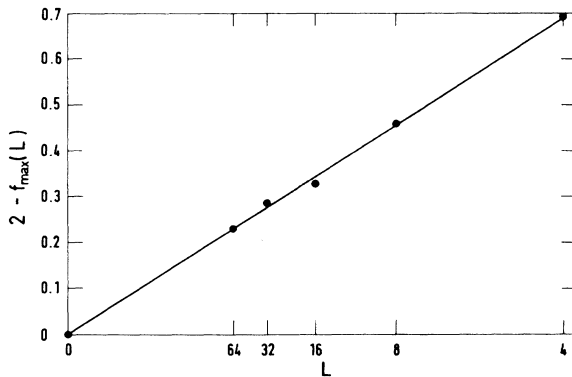


FIG. 14. $2 - f_{\max}$ against $1/\log L$ for $x=0$, $q=1$ and an externally applied elongation.

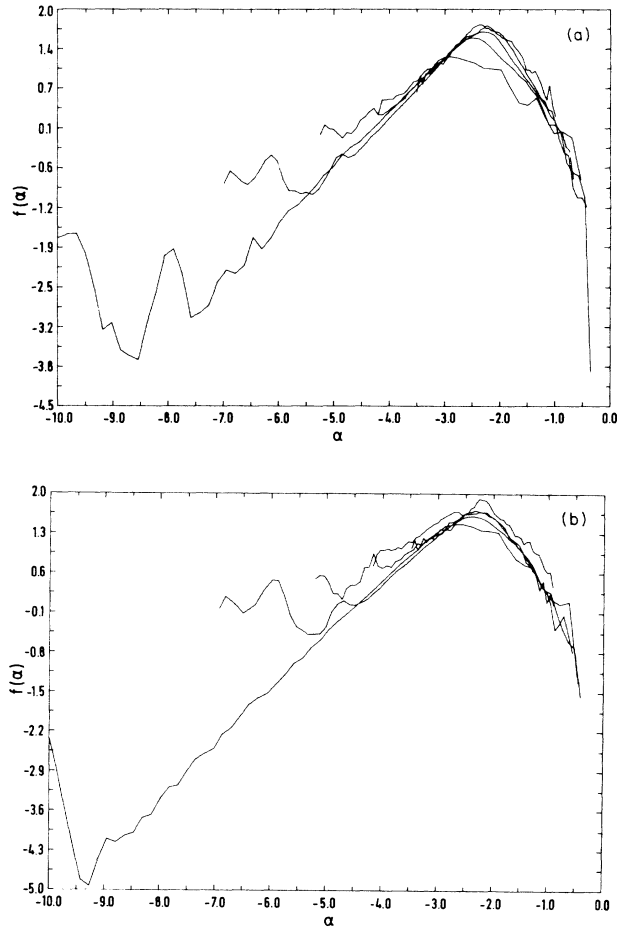


FIG. 15. Spectrum $f(\alpha)$ for the distribution $n(S)$ of shears S . We show data for $L=4, 8, 16, 32$, and 64 . For externally applied elongation, $q=1$ and (a) $x=0$, $c_1=1.5$, $c_2=1.0$; (b) $x=0.5$, $c_1=1.6$, $c_2=1.5$.

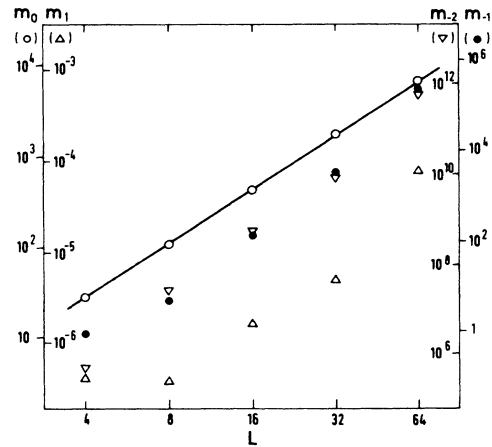


FIG. 16. Log-log plot of the moments of the force distribution $n(F)$ for the case $x=0$, $q=1$ and external elongation as function of L .

4 also in agreement with our expectations. Already $k = 1$ and $k = -2$ give unclear results not only because of statistical fluctuations but also because Eq. (14) is a sum of very large and very small numbers giving rise to roundoff errors. This can be understood if one considers the enormous variation in the local forces seen, e.g., in Fig. 10. We conclude that in this case the moments are not a good tool to investigate multifractality.

V. CONCLUSION

We simulated the rupture of an elastic network with random breaking thresholds. Three regimes can be distinguished: First, the controlled regime dominated by disorder, then the brittle threshold where the maximum external force must be applied, and finally the catastrophic regime where statistical fluctuations are very strong.

In the controlled regime we found that force f and displacement λ at the breaking of a beam scale with the system size L like a powerlaw with an exponent which for both is numerically very close to $3/4$ nearly independent of the distribution of thresholds or the externally applied strain. The number n of broken beams scales with an exponent of about $7/4$ so that a relation

$$f \propto \lambda \propto n/L \quad (16)$$

is numerically verified. Physically this means that the displacement depends roughly only on the density of broken beams along a line across the network.

For the number n_b of beams that must be broken to reach the maximum in the force and thus trigger off the catastrophe we found a powerlaw dependence on L with the same exponent around $7/4$. In the scalar case two different approximations have been proposed for this brittle regime: the single crack approximation,⁸ i.e., the approximation that any crack larger than one lattice unit is unstable, yields $n_b \propto L$. The dilute crack approximation,⁷ in which cracks are like random percolation at low concentration, gives if Eq. (16) is used $n_b \propto L^2/\sqrt{\ln L}$. Our result $n_b \propto L^{7/4}$ lies between the two. We think that the essential effect that both approximations overlook is that once a crack starts growing it can be, and usually is,

stopped again in its growth due to the encounter with a region of stronger beams.

In the catastrophic regime we focused on the last configuration of the lattice before it falls apart. The tenuous structure of the stress-carrying part of the lattice induces multifractality in the distribution of local strains, which can be visualized in the $f(\alpha)$ spectrum.

As a result we have several predictions that one should in principle be able to verify experimentally. There are on one hand the scaling laws of Eqs. (10) and (11) as well as the size dependence of Fig. 8 which one should be able to see in experimental settings like the one described in Ref. 23. Multifractality is more difficult to verify, however, photoelasticity might be a tool to do so.

Our system of beams as well as the way we introduce the disorder imply a certain number of restrictions on the applicability of our model to rupture phenomena. Other versions like a central force model²⁴ or a scalar model²⁵ have also been studied and the conclusions found are similar to the ones found in this work giving strong support nevertheless that our results are quite generic. It would, of course, be interesting to investigate the theoretical principles underlying this universal behavior.

In reality many other effects will occur during a rupture due to the various properties of the materials. Let us mention here only one: plasticity. Efforts have also been made to understand the behavior of materials made of fibers via thermally activated thresholds.²⁶

Of course, the most urgent thing to do next in order to describe the experimental reality of breaking is to study the three-dimensional behavior. Work in this direction is under way.

ACKNOWLEDGMENTS

It is a pleasure to acknowledge useful discussions with E. Guyon. We are indebted to M. Novotny, and IBM Bergen Scientific Centre, for their hospitality in Bergen where most of the computations were performed on an IBM 3090. S.R. is supported by an ATP contract of the CNRS and A.H. by the SFB125.

¹See, e.g., H. D. Bui, *Mécanique de la Rupture Fragile* (Masson, New York, 1978); B. R. Lawn and T. R. Wilshaw, *Fracture of Brittle Solids* (Cambridge University Press, Cambridge, 1975) or the collection of articles in *Fracture*, Vols. I–VII, edited by H. Liebowitz (Academic, New York, 1984); in *Fragmentation, Form and Flow in Fractured Media*, Vol. 8 of *Annals of the Israeli Physical Society*, edited by R. Englman and Z. Jaeger (Hilger, London, 1986).

²P. G. de Gennes, *J. Phys. (Paris) Lett.* **37**, L1 (1976).

³S. Feng and P. N. Sen, *Phys. Rev. Lett.* **52**, 216 (1984); Y. Kantor and I. Webman, *ibid.* **52**, 1891 (1984); S. Alexander, *J. Phys. (Paris)* **45**, 1939 (1984); A. Hansen and S. Roux (unpublished).

⁴H. Takayasu, *Phys. Rev. Lett.* **54**, 1099 (1985).

⁵M. Sahimi and J. D. Goddard, *Phys. Rev. B* **33**, 7848 (1986).

⁶L. de Arcangelis, S. Redner, and H. J. Herrmann, *J. Phys.*

(Paris) Lett. **46**, L585 (1985); A. Gilabert, C. Vanneste, D. Sornette, and E. Guyon, *J. Phys. (Paris)* **48**, 763 (1987).

⁷P. M. Duxbury, P. D. Beale, and P. L. Leath, *Phys. Rev. Lett.* **57**, 1052 (1986); P. M. Duxbury, P. L. Leath, and P. D. Beale, *Phys. Rev. B* **36**, 367 (1987).

⁸B. Kahng, G. G. Batrouni, S. Redner, L. de Arcangelis, and H. J. Herrmann, *Phys. Rev. B* **37**, 7625 (1988); the limit of infinite disorder has been treated in S. Roux, A. Hansen, H. J. Herrmann, and E. Guyon, *J. Stat. Phys.* **52**, 251 (1988).

⁹P. M. Duxbury and P. L. Leath, *J. Phys. A* **20**, L411 (1987).

¹⁰J. Machta and R. M. Guyer, *Phys. Rev. B* **36**, 2142 (1987); Y. S. Li and P. M. Duxbury, *ibid.* **36**, 5411 (1987); B. Kahng, G. G. Batrouni, and S. Redner, *J. Phys. A* **20**, L827 (1987).

¹¹P. Meakin, *Thin Solid Films* **151**, 165 (1987).

¹²L. Niemeyer, L. Pietronero, and H. J. Wiesmann, *Phys. Rev. Lett.* **52**, 1033 (1984).

- ¹³E. Louis and F. Guinea, *Europhys. Lett.* **3**, 871 (1987).
- ¹⁴S. Roux and E. Guyon, *J. Phys. (Paris) Lett.* **46**, L999 (1985).
- ¹⁵See e.g., R. J. Roark and W. C. Young, *Formulas for Stress and Strain* (McGraw-Hill, Tokyo, 1975), p. 89 or S. Timoshenko, *Strength of Materials* (Van Nostrand, Princeton, 1946), Vol. II.
- ¹⁶J. Salençon, *Calcul à la Rupture et Analyse Limite* (Presses de l'ENPC, Paris, 1983), p. 110.
- ¹⁷G. G. Batrouni, A. Hansen, and M. Nelkin, *Phys. Rev. Lett.* **57**, 1336 (1986).
- ¹⁸G. G. Batrouni and A. Hansen, *J. Stat. Phys.* **52**, 747 (1988).
- ¹⁹L. de Arcangelis, S. Redner, and A. Coniglio, *Phys. Rev. B* **31**, 4725 (1985); **34**, 4656 (1986); R. Rammal, C. Tannous, P. Breton, and A. M. S. Tremblay, *Phys. Rev. Lett.* **54**, 1718 (1985).
- ²⁰T. C. Halsey, P. Meakin, and I. Procaccia, *Phys. Rev. Lett.* **56**, 854 (1986); T. C. Halsey, M. H. Jensen, L. P. Kadanoff, I. Procaccia, and B. I. Shraiman, *Phys. Rev. A* **33**, 1141 (1986).
- ²¹L. de Arcangelis, in *Proceedings of the Summer School Cargèse, 1987* (unpublished); G. Paladin and A. Vulpiani, *Phys. Rep.* **156**, 147 (1987).
- ²²G. G. Batrouni, A. Hansen, and S. Roux, *Phys. Rev. A* **38**, 3820 (1988).
- ²³L. Benguigui, P. Ron, and D. J. Bergman, *J. Phys. (Paris)* **48**, 1547 (1987).
- ²⁴A. Hansen, S. Roux, and H. J. Herrmann (unpublished).
- ²⁵L. de Arcangelis and H. J. Herrmann (unpublished).
- ²⁶Y. Termonia, P. Meakin, and P. Smith, *Macromolecules* **18**, 2246 (1985).